1521-009X/47/11/1232–1239$35.00
Drug Metabolism and Disposition

https://doi.org/10.1124/dmd.119.088732
Drug Metab Dispos 47:1232–1239, November 2019

Kinetic Modeling of Steady-State Situations in Cytochrome P450 Enzyme Reactions[S]

F. Peter Guengerich

Department of Biochemistry, Vanderbilt University School of Medicine, Nashville, Tennessee

Received July 12, 2019; accepted August 14, 2019

ABSTRACT

In the course of investigations of the kinetics of individual reactions of cytochrome P450 (P450) enzymes, a number of points about the complexity of P450 enzyme kinetics have become apparent. Several of these are of particular relevance to work with P450 enzymes in the course of drug development and lead optimization, particularly with regard to estimating in vitro kinetic parameters and dealing with enzyme inhibitors. Modern simulation modeling has been applied to situations involving issues of preincubation time with moderate strength and strong inhibitors, inhibition by tightly bound ligands that have been identified in P450 enzymes, extensive substrate depletion, P450 reactions with a rate-limiting step after product formation, and the consumption of an inhibitor during a reaction by either a P450 enzyme being monitored or another one in a mixture. The results all follow from first principles, and simulations reveal the extent of their significance in various settings. The order of addition of substrate and inhibitors can change the apparent outcome (inhibition constant, K_i), and the effect of the order is more pronounced with a stronger inhibitor. Substrate depletion alters parameters (Michaelis constant, K_m) and can generate apparently sigmoidal plots. A rate-limiting step after product formation lowers the apparent K_m and distorts K_i. Consumption of an inhibitor during a reaction affects K_i and differs depending on which enzyme is involved. The results are relevant with P450 enzymes and other enzymes as well.

SIGNIFICANCE STATEMENT

Kinetic simulations have been used to address several potential problems in enzyme kinetic analysis. Although the simulations done here are general for enzyme reactions, several problems addressed here are particularly relevant to cytochrome P450 reactions encountered in drug development work.

Introduction

Many in vitro assays are performed with human cytochrome P450 enzymes in the course of modern drug development (Zhang et al., 2008; Pearson and Wienkers, 2019). The approach has been highly successful, in general, in allowing extrapolation of parameters to generate estimates of in vivo pharmacokinetics (Polasek et al., 2018; Wakayama et al., 2018). Another major goal of in vitro work is with P450 inhibitors, largely in the context of predicting drug-drug interactions (Rodrigues and Lin, 2001; Wienkers and Heath, 2005; McGinnity et al., 2008; Guest et al., 2011; Guengerich, 2019).

However, there are several issues with the design of in vitro experiments, the meaning of individual kinetic parameters, and the interpretation of what some parameters really mean. One parameter of considerable interest is k_{cat}/K_m (or V_{max}/K_m), termed the specificity constant by biochemists (Johnson, 2003, 2019) and in vitro clearance (Cl_{int}) by pharmacologists. There are also issues in the evaluation of inhibition results, not only time-dependent (mechanism-based) but even the simpler pure competitive inhibition.

In the course of our kinetic studies with several human P450 enzymes, we have been using kinetic modeling/fitting software, including KinSim (Bell and Guengerich, 1997), DynaFit (Guengerich et al., 2002), and most recently KinTek Explorer (Chowdhury *et al.*, 2010; Guengerich *et al.*, 2019a,b; Reddish and Guengerich, 2019). Most of our work has been done in fitting experimental data, but the software can also be very useful in modeling possible outcomes of experimental situations, sometimes leading to a preferred approach.

Several issues could potentially be considered, but these were the five areas investigated: 1) the effect of the order of mixing substrate and inhibitor with an enzyme, including the length of preincubation time, 2) the effect of a very tightly bound ligand on enzyme kinetics, 3) the effect of substrate depletion, 4) the effect of a rate-limiting step after product formation, and 5) issues related to changes in inhibitor concentration due to biotransformation by the same enzyme or another in a mixture (e.g., microsomes). The modeling is generic for enzymes but highly relevant to P450 enzymes.

Materials and Methods

All kinetic simulations were performed in KinTek Explorer software (version 8.0; KinTek Corp., Snow Shoe, PA) using an Apple iMac OSX 10.13.6 system. GraphPad Prism v. 8.0 (GraphPad, San Diego, CA) was used for some of the fitting: plots of rates or products formation versus substrate concentration (specifically Fig. 2C, Fig. 3C, Fig. 4, B and C, Fig. 5B, Fig. 6D, and Fig. 8C).

The system used in all simulations was a two-stage mixing model (Supplemental Figs. 1–8). The enzyme E was present in the first time component (t_1 step), with or without an inhibitor, with this "preincubation" time (t_1) varying as described. The enzyme (E) was then mixed (t_2 step) with multiple concentrations of substrates (S),

This work was supported by National Institutes of Health Grant R01 GM118122 (F.P.G.).
https://doi.org/10.1124/dmd.119.088732.
[S]This article has supplemental material available at dmd.aspetjournals.org.

ABBREVIATIONS: CI, confidence interval; E, enzyme; EP, enzyme-bound product; I, inhibitor; k_{cat}, maximum velocity for an enzyme reaction; K_d, dissociation constant; K_i, inhibition constant; K_m, Michaelis constant (substrate value at which half-maximal velocity is achieved); P, product; P450 (or CYP), cytochrome P450; S, substrate.

and the product (P) was monitored as a function of time (generally 180 seconds = 3 minutes). The substrate, enzyme, inhibitor concentrations, and reaction time were selected to reflect typical values that might be encountered in assays in the pharmaceutic industry.

All steady-state K_i values were calculated using a simple competitive inhibition equation (Segel, 1975):

$$K_{m,apparent} = \frac{K_m[I]}{K_i} + K_m$$

Most values are rounded to two significant digits.

Results

General Design of Simulations. Rates of binding of molecules to enzymes were generally set to 10^6 M^{-1} s^{-1} (1 μM s^{-1}). This value is in the range of values we have measured for human P450 enzymes (Guengerich et al., 2019b). (Multiphasic binding is simplified here for the modeling.) This rate constant is in the range generally accepted for enzyme-ligand binding (Schreiber et al., 2009); higher rates (e.g., 10^8–10^9 M^{-1} s^{-1}) usually result from the influence of charges (Fersht, 1999; Zang et al., 2005; Schreiber et al., 2009; Guengerich et al., 2019b).

The final enzyme concentration in the assay was generally set to 0.05 μM, which is realistic in the context of many sensitive assays done today using liquid chromatography with mass spectrometry methods, much less than earlier assays done with colorimetric assays (e.g., 1 to 2 μM) (Guengerich, 2014). Most of the simulations were done with a range of substrate concentrations varying from 0.5 to 100 μM. The modeling also focused on K_i values in the range of 1 nM–10 μM, which are likely to be of most concern with P450 enzymes in drug development.

Effects of Preincubation Time with Inhibitors. The first model used a K_i inhibitor (I) (1 μM) with with a 0.1 μM K_d value (Fig. 1). When there was no preincubation period (i.e., I was added along with S to start the reaction), a brief faster reaction was seen (most easily at the highest S concentration) before the reaction was linear (Fig. 1B). However, when the preincubation was performed with the inhibitor present for 120 seconds (Fig. 1C), there was a noticeable lag phase before the substrate displaced the inhibitor and the steady-state (linear reaction) occured (again, most easily seen at the highest concentration).

In the two analyses (Fig. 1, B and C), the respective k_{cat} values were 0.0098 seconds and 0.0089 s^{-1} (compared with 0.0097 s^{-1} in the uninhibited reaction). The respective K_i values (in Fig. 1, B and C) were 0.064 and 0.071 μM, both only slightly lower than the K_d of 0.1 μM set for I in the model.

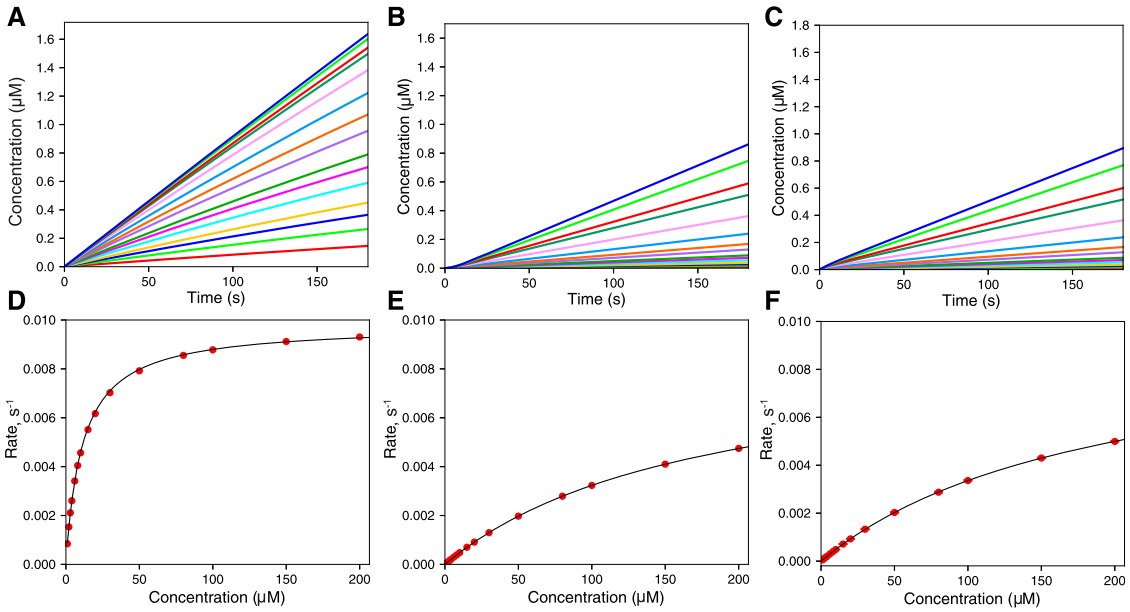

Fig. 1. Effect of preincubation time with an enzyme inhibitor. The kinetic model consisted of:

Step	Reaction	k_+	k_-	K_d
1	E + S ⇄ ES	1 μM^{-1} s^{-1}	10 s^{-1}	10 μM
2	ES → EP	0.1 s^{-1}	—	
3	EP ⇄ E + P	2 s^{-1}	1 μM^{-1} s^{-1}	2 μM
4	E + I ⇄ EI	1 μM^{-1} s^{-1}	0.1 s^{-1}	0.1 μM

with [E] = 0.1 μM mixed with [S] = 1, 2, 3, 4, 6, 7, 10, 15, 20, 30, 50, 80, 100, 150, and 200 μM, to yield final concentrations of one-half of these (see Supplemental Information). (A) No inhibitor added. (B) [I] = 2 μM added in preincubation for 0.1 seconds. (C) [I] = 2 μM added in preincubation for 120 seconds, final [I] = 1 μM after mixing to initiate the reaction. The following parameters were estimated in each part:

Part	k_{cat} (s^{-1})	$K_{m,(app)}$ (μM)	K_i (μM)
A	0.0097	11.5	—
B	0.0098	190	0.064
C	0.0089	175	0.071

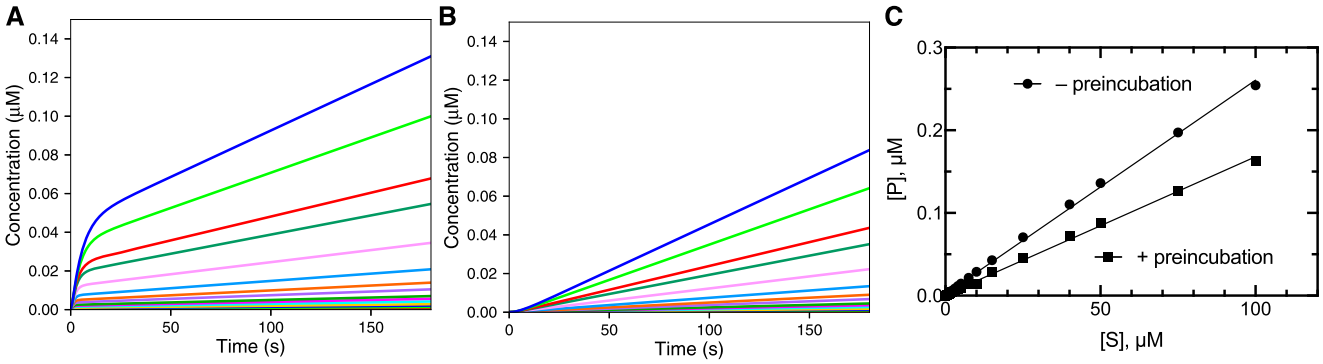

Fig. 2. Effect of preincubation time and a strong enzyme inhibitor. The kinetic model was the same as in Fig. 1, except that k_{-4} was 0.01 s^{-1} (K_d 10 nM). I was added at 2 μM for a final concentration of 1 μM in the reaction. (A) Zero preincubation time with inhibitor before adding substrate. (B) Preincubation time of 30 seconds before adding substrate. (C) Final product concentrations after 180 seconds produced in parts A (●) and B (■). In part C, the slope of the linear fit plot derived without preincubation was 0.00269 ± 0.00003 (S.E.M.), r^2 0.9986; and the slope of the linear fit plot derived with preincubation was 0.00167 ± 0.00002 (S.E.M.), r^2 0.9978.

The effect of preincubation time and order was also examined with a 10-fold stronger inhibitor (K_d 10 nM set in model). The "burst" (Fig. 2A) and lag (Fig. 2B) were clearly observable and are more pronounced than in Fig. 1, as might be expected. The patterns shown in Fig. 2A were very similar to the reactions in which the rate-limiting step occured after product formation (as discussed later). As in Fig. 1, time is needed for either the inhibitor to replace the substrate and act (Fig. 2A) or for the substrate to replace the inhibitor (Fig. 2B) and be acted upon by the enzyme.

The rates in these reactions could not be accurately fit by linear extrapolations (especially Fig. 2A), so the concentration of product measured at 180 seconds reaction time (3 minutes) was used as a surrogate of the rate. This measurement would correspond to a value determined by liquid chromatography with tandem mass spectrometry typically measured in such a kinetic screen. The plots (vs. [S]) are not saturating in either case (Fig. 2C), in keeping with the very low K_i (which could not be estimated by the usual criteria; see *Materials and Methods*). It should be noted that the rates ([P] formation) measured after preincubation with the inhibitor present (120 seconds) will ultimately reach those with the inhibitor added at the same time as the substrate but not within the 180-second reaction time.

A conclusion of the modeling presented here is that, in general, preincubation with both substrate and inhibitor is preferred, particularly if the inhibitor is tightly bound. In robotic systems, this design should be incorporated. If crude systems are used (e.g., microsomes), it is conceivable that the order of addition might be influenced by the instability of an inhibitor, such as an esterase substrate (see the section *Issues with Consumption of an Inhibitor during Incubations* for that case).

Effect of a Very Tightly Bound Ligand on Reaction Rates. The general concept of a very tightly bound inhibitor was examined. This case corresponds to recombinant P450 enzymes that are purified but still contain a ligand. Several examples of such behavior have been reported, including fatty acids in P450 2C8 (Schoch et al., 2004) and bacterial P450 119A1 (Krest et al., 2013) and indole in P450 2A13 (Smith et al., 2007). Although the cited publications regarding these preparations were of interest due to structural or mechanistic aspects, the point we have addressed is that catalytic assays would be very problematic.

A related concern is purified P450 preparations that have been prepared in the presence of strong ligands to stabilize the enzyme during expression or purification, such as family 1A P450 enzymes (Sandhu et al., 1994; Sansen et al., 2007; Wang et al., 2011). With these enzymes, the presence of residual inhibitor may have to be critically analyzed to permit careful studies on catalysis or inhibition. Although they are not generally considered to be high affinity, nonionic detergents (Hosea and Guengerich, 1998) and ionic steroidal detergents (Hobler *et al.*, 2012; Reddish and Guengerich, 2019) may be present in P450 enzymes and produce artifacts of this nature.

In this model, a K_d of 1 nM was arbitrarily set, with [E] = 0.05 μM and one inhibitor present (in the t_2 phase, after 2-fold dilution of enzyme to start the reaction, i.e., [E] = 0.10 μM in t_1 phase). The quadratic analysis indicated that ~90% of the enzyme would be bound to I, so the simulation was initiated with a mixture of 0.09 μM [EI], 0.01 μM $[E]_{free}$, and 0.01 μM $[I]_{free}$ in the t_1 phase. The rate plots were concave upward, due to the time required for the substrate to replace I (Fig. 3A). Although the linear fits (Fig. 3A) were not perfect, the results yielded a reasonable hyperbolic plot versus [S] (Fig. 3B). A more accurate inhibition plot was seen when [P] (at 180 seconds) was plotted versus [S] (Fig. 3C). In the latter analysis, the K_m apparent was 16 μM, and K_i was estimated to be 71 nM, two orders of magnitude greater than the set K_d for I (1 nM).

Interestingly, k_{cat} was also only 15% of the value obtained in the absence of inhibitor, although this model is one involving competitive inhibition.

Effects of Substrate Depletion. We also used same basic model (Fig. 1) but with the final enzyme concentration ([E]) increased 40-fold (to 2 μM) to run the reaction at lower substrate concentrations to completion (Fig. 4A). As expected, in the reactions at lower [S] all of the substrates had been converted to product; even with the higher substrate concentrations, the reactions were no longer linear.

The plots (Fig. 4A) did not fit well to linear equations, so product formation ([P]) at t = 180 seconds was plotted versus [S] (Fig. 4B). As expected, the plot was not saturating, but a K_m value of 64 μM could be estimated (6.4-fold > K_d). When enzyme-bound product (EP) was included, the totals were expectedly higher (Fig. 4B), and a K_m of 34 μM was estimated.

When the initial phase of the reaction was plotted, the results with [P] generated an apparent sigmoidal curve (Fig. 4C). Many reports of Hill plots with low n values (1.1–1.5) have been reported in the literature, especially for P450 3A4, including some of our own (Ueng et al., 1997; Korzekwa et al., 1998; Fowler et al., 2002; Frank et al., 2011). Analysis of the [P]-only data (Fig. 4B) yielded a Hill n value of 1.11 (95% confidence interval [CI], 1.05–1.17). Use of only the [P] points shown in Fig. 4C yielded n = 1.42 (CI, 1.37–1.47) (and S_{50} = 40 μM). However, when the sum of [E] + [EP] is considered, the sigmoidicity is lost (Fig. 4C).

The extent to which this phenomenon is responsible for weak Hill plots in the literature is unknown, in that few describe details of reaction conditions. If the sum of [EP] + [P] is considered, then even running

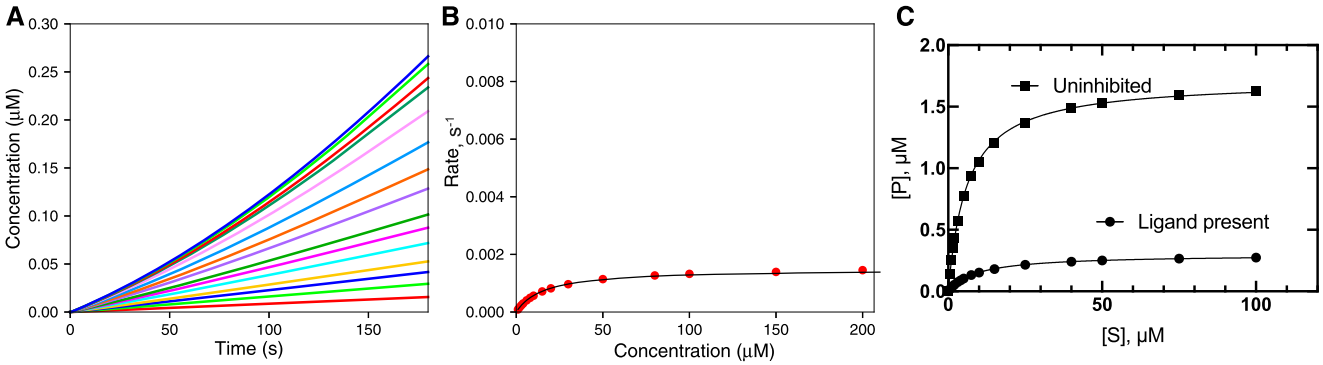

Fig. 3. Effect of a very tightly bound ligand on an enzyme reaction. The model used in Fig. 1 was applied, without any preincubation. Here, [I] was set equal to [E], 0.1 μM, both diluted to 0.05 μM in the reaction. At this concentration of [E] and [I] and K_d for the EI complex set at 1 nM (k_{-4} = 0.001 μM in model for Fig. 1), a quadratic equation indicates that ~90% of the E is bound as EI, so the reaction began with [EI] = 0.09 μM, $[E]_{free}$ = 0.01 μM, and $[I]_{free}$ = 0.01 μM, mixed with substrate. (A) Time course of reaction at varying substrate concentration. (B) Plot of apparent line fits of rates (part A) versus [S]. (C) Final concentration of product P formed in part A (●) compared with uninhibited reaction ([I] = 0) (Fig. 1A), fit to Michaelis-Menten plot. In part C the $k_{cat,apparent}$ was 0.0015 s^{-1} (compared with 0.0097 s^{-1} in Fig. 1A), $K_{m,apparent}$ was 16 μM, and K_I was estimated to be 71 nM (compare with k_{-4}/k_5 = 1 nM in the model setup). The r^2 values were 0.9997 for the uninhibited reaction and 0.9998 for the inhibited reaction.

reactions to completion cannot give a sigmoidal curve, at least in the simplest case, in that doubling [S] can only double ([P] + [EP]) and a linear fit will be seen (Fig. 4C).

In practice, running an assay in which the reaction was quenched with a solvent (or acid) to release the enzyme-bound product would yield P + EP (Fig. 4, B and C) and solve the problem. However, in a continuous spectrophotometric (or fluorimetric) assay this would not be the case, and the caveats could apply.

Issues with a Rate-Limiting Step after Product Formation. This is a classic situation seen in enzyme kinetics (Walsh, 1979) and has also been identified in some P450 reactions. It is best documented in the cases of oxidation of ethanol and acetaldehyde by P450 2E1 (Bell and Guengerich, 1997; Bell-Parikh and Guengerich, 1999), but less definitive cases have also been reported such as toluene (rat liver microsomes, P450 unknown) (Ling and Hanzlik, 1989) and 18-hydroxycorticosterone (bovine P450 11B1) (Imai et al., 1998).

Such reactions are characterized by burst kinetics (Fig. 5A), with the sharpness of the burst depending upon the relative rates of individual reaction steps. In the modeling in Fig. 5A, step 3 was reduced to 0.02 s^{-1} (10-fold). Such plots are usually fit to $v = Ae_1^{t-k} + k_{ss}$ [S], where A is a constant, k_{ss} is a steady-state rate, and k_1 is an exponential (Johnson, 2003). A linear fit of Fig. 5A is not possible, and [P] at 180 seconds was used as before (Fig. 5B).

As expected, the sum ([EP] + [P]) was higher than [P] in that much of the product remained bound. The k_{cat} value was ~20% of that observed when k_3 = 2 s^{-1} (Fig. 3C) although the rate constant had been reduced 10-fold. The estimated K_m was 4.0 μM when only [P] was considered and was 2.1 μM when both [P] and [EP] were considered, compared with K_d = 10 μM for binding substrate in the model. The relationship $K_m < K_d$ is a classic phenomenon when product release is rate limiting (Walsh, 1979; Guengerich et al., 2003).

Another issue is the nature of competitive inhibition when the rate-limiting step follows product formation (Fig. 6). The model used in Fig. 5 was used with [I] = 1 μM, and the K_d of I was set at 0.1 μM (with a preincubation time of 120 seconds) (Fig. 6A). The burst character is still obvious, at least at the higher substrate concentrations. Although linear fits of the traces were less than ideal (Fig. 6B), the rate plots generated a hyperbolic fit (Fig. 6C), with k_{cat} = 0.0019 s^{-1} and $K_{m,apparent}$ 21 μM, yielding K_i = 0.95 μM. The plot of [P] (t = 180 seconds) versus [S] gave a $K_{m,apparent}$ value of 11 μM, yielding K_i = 0.23 μM. These K_i values differ and can be compared with the K_d of 0.1 μM set in the model.

Issues with Consumption of an Inhibitor during Incubations. One issue with an enzyme inhibitor is that it is also a molecule and subject to reaction. This can manifest in a role as a competitive inhibitor —that is, to be transformed (to a noninhibitory molecule) by the enzyme under investigation. A model was developed in which the enzyme

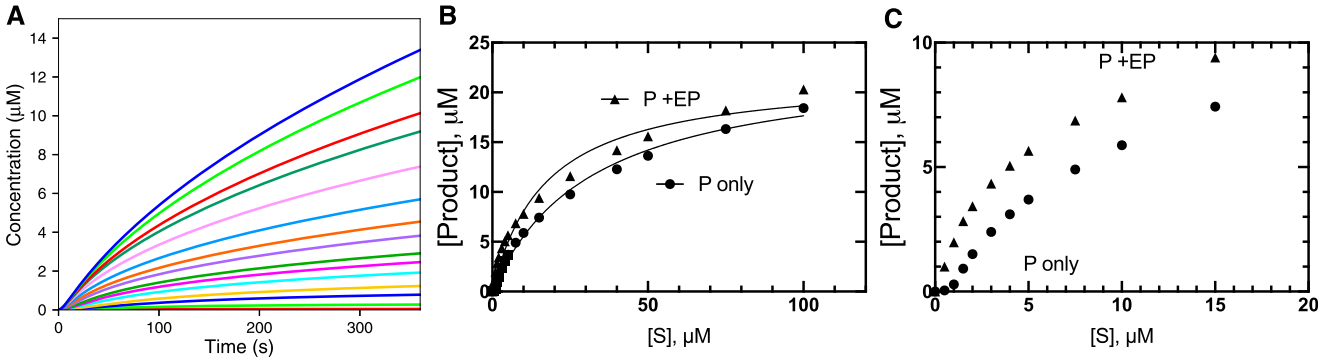

Fig. 4. Effect of long reaction time and substrate depletion on kinetic parameters. The starting concentration of [E] was raised to 4 μM (final [E] = 2 μM). (A) Plot of [P] versus time at varying substrate concentrations. (B) [P] at 180 seconds plotted versus [S] (● [P] only, ▲ [P] + [EP]). (C) Expansion of plot from part B in low [S] region. The $K_{m,apparent}$ values were 64 μM for P only and 34 μM for P + EP. In part B, the r^2 values (hyperbolic fit) were 0.9783 for [P] + [EP] and 0.9947 for [P] only. In part C, the r^2 value (Hill equation, sigmoidal fit) was 0.9978 for [P] only.

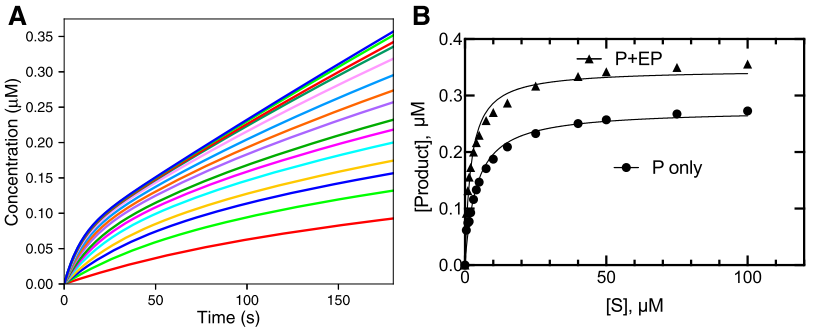

Fig. 5. Effect of a rate-limiting step after product formation. The basic model in Fig. 1 was used, except k_3 was reduced to 0.02 s^{-1} (10-fold). (A) Plots of product formation versus Time at varying concentrations of substrate. (B) Plots of product formation versus [S] for [P] only (●) and the sum of [P] + [EP] (▲). The K_m value for P only was 4.0 μM, and the K_m for (P + EP) was 2.1 μM (compared with K_d = 10 μM for S in model). In part C, the r^2 values (hyperbolic fit) were 0.9835 for [P] + [EP] and 0.9820 for [P] only.

reacted with the inhibitor (I) at the same rate as the substrate (S) and was then released from the enzyme (step 5 in Fig. 7). The result of the transformation of the inhibitor can be seen in comparing Fig. 7, B and C. The course of the disappearance of I is shown in Fig. 7D, with less inhibitor being removed at higher concentrations of the substrate due to competition. In this model, the calculated K_i was 0.13 μM without inactivation of I (Fig. 7B) but rose to 0.70 μM in Fig. 7C when it was transformed (compare K_d of 0.10 μM for I set in the model). For this, k_{cat} was nearly identical in all situations (Fig. 7).

Another situation occurs with mixtures of P450 enzymes in microsomes when an inhibitor of one P450 is being oxidized by another P450; for instance, quinidine is an inhibitor of P450 2D6 but a substrate for P450 3A4 (Guengerich et al., 1986). Such a model was set up, with a second enzyme (F) transforming I as rapidly as E transforms S (Fig. 8). As in Fig. 7C, there is curvature in the plots of [P] versus time, as I is removed from inhibiting E, but the degree is more marked (Fig. 8A). A plot of the course of I during the reaction shows only a limited effect of S on the course of I, as expected and in contrast to Fig. 7D (Fig. 8B). A hyperbolic plot of [P] (at t = 180 seconds) versus [S] yielded k_{cat} = 0.0089 s^{-1} (near the uninhibited value) and K_I = 5.2 μM, 52-fold > K_d for I (0.1 μM) (Fig. 8C).

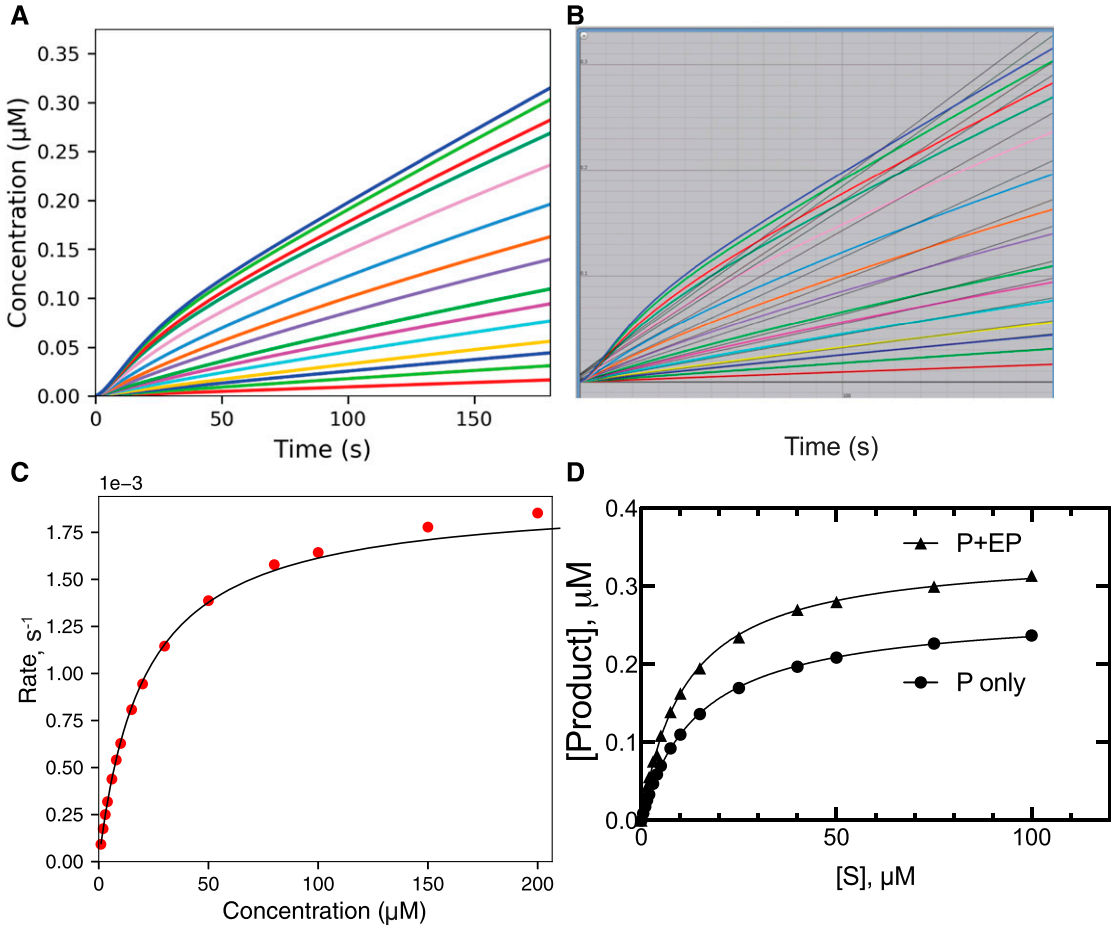

Fig. 6. Inhibition of an enzyme with a slow step after product formation. The model of Fig. 5 (Fig. 1 with k_3 = 0.02 s^{-1}) was used with [I] = 1 μM, k_4 = 1 μM^{-1} s^{-1}, and k_{-4} = 0.1 $second^{-1}$ (K_d for I = 0.1 μM). The preincubation time with I was 120 seconds. (A) Plot of [P] versus Time. (B) Linear fits to curves in part A. (C) Rate versus [S] (rates from part B). (D) Plots of total product formed after 180 seconds versus [S]: [P] only (●) and [P] + [EP] (▲). The k_{cat} was 0.0019 s^{-1}, $K_{m,apparent}$ was 21 μM, and K_i was 0.95 μM (compared with K_d = 0.1 μM in model). In part C, the r^2 values (hyperbolic fit) were 0.9999 for [P] + [EP] and 0.9992 for [P] only.

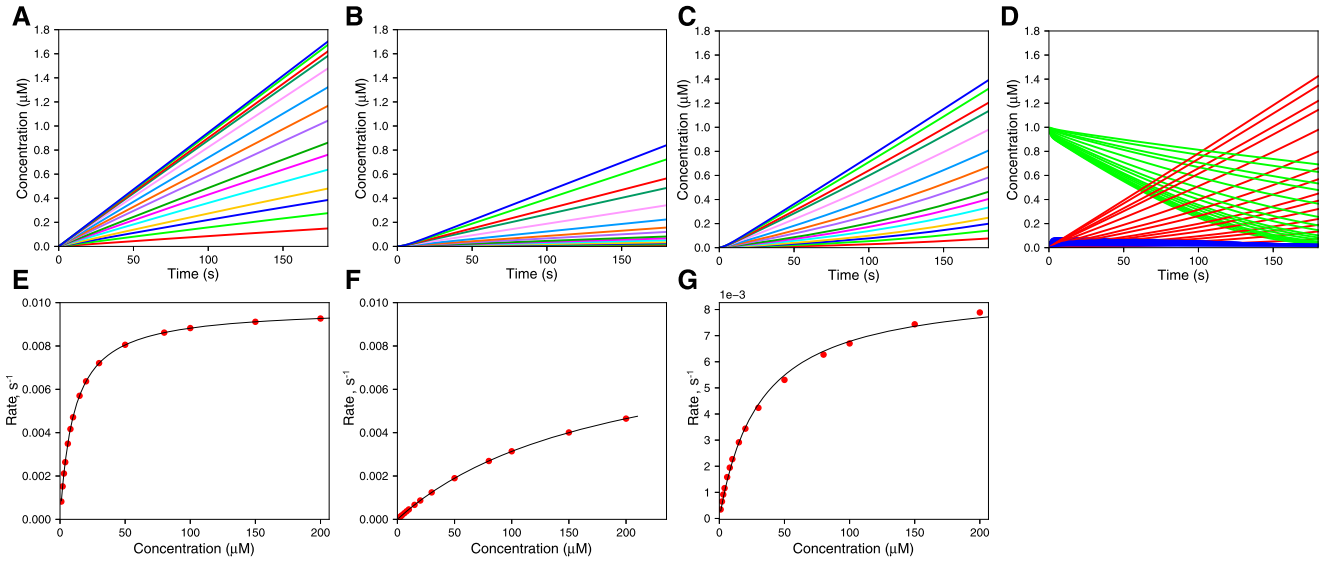

Fig. 7. Effect of consumption of inhibitor by an enzyme. The basic model of Fig. 1 was used, with Step 5 added in Part C.

Step	Reaction	k_+	k_-	K_d
1	E + S ⇄ ES	1 μM^{-1} s^{-1}	10 s^{-1}	10 μM
2	ES → EP	0.1 s^{-1}	—	
3	EP ⇄ E + P	2 s^{-1}	1 μM^{-1} s^{-1}	2 μM
4	E + I ⇄ EI	1 μM^{-1} s^{-1}	0.1 s^{-1}	0.1 μM
5	EI → E + X	0.1	0	

(A) Plot of P versus Time at varying concentrations of X. (B) Same as in part A but with [I] = 2 μM in Premix, $k_5 = 0$. (C) Same as in Part B but with $k_5 = 0.1$ s^{-1} (same as k_2). No correction was made for a product of I binding to E. (D) Time course of [P] (red), [I] (green), and [EI] during reaction (in part C). (E) The v versus [S] plot for part A. (F) The v versus [S] plot for part B. (G) The v versus [S] plot for part C. The following parameters were estimated:

Part	k_{cat} (s^{-1})	$K_{m,apparent}$ (μM)	K_i	$K_{d(S)}$	$K_{d(I)}$
A	0.0098	10.6	—	10	—
B	0.0090	187	0.13	—	0.10
C	0.0089	30	0.70	—	0.10

Discussion

Several relevant scenarios related to P450 enzymes were examined by modeling. The results all follow from first principles, but some of the findings may not be so obvious, particularly for individuals who are not acquainted with enzyme kinetics. Modeling using modern software allows ready prediction of some issues in kinetics.

One aspect not dealt with here but highly relevant is the use of a relatively new approach to fitting actual v versus S plots—that is, Michaelis-Menten kinetics. The original publication (Michaelis and Menten, 1913, 2013; Michaelis et al., 2011) did not estimate K_m directly, as was done by Lineweaver and Burk (1934) and elsewhere. It can be argued, and I definitely agree, that the two major parameters in steady-state enzyme kinetics are k_{cat} (V_{max}) and k_{cat}/K_m (Northrop, 1998), the latter of which Johnson terms k_{sp} (specific constant) (Johnson, 2019).

Mathematically, the error is reduced in using a program to solve for k_{cat} and k_{sp} (k_{cat}/K_m)—and then deriving K_m from the quotient. The process can easily be performed in GraphPad Prism software using the equation

$$Y = (ksp*X)/(1 + (ksp*X/kcat))$$

which we now do routinely in this laboratory. The error (e.g., S.D.) is reduced in all cases compared with calculating k_{cat} and K_m and then dividing. However, this approach was not used in this study because all the data are synthetic (modeling).

The issue of the correct prediction of K_i may or may not be an issue in predicting enzyme inhibition. Very weak and very strong inhibitions are easy to spot regardless of the assays; however, in borderline cases, providing the most accurate K_i (or at least EC_{50}) may be critical to correct prediction, even with only competitive inhibition.

The simulations presented in this study are relatively simple, with an enzyme only binding to a single substrate (S) or inhibitor (I), and the rate constants for binding and release of S, I, and product (P) varying. However, P450 reactions can be much more complex. Heterotropic cooperativity (i.e., activation) was recognized nearly 50 years ago (Wiebel et al., 1971; Buening et al., 1978; Huang et al., 1981) and homotropic cooperativity ≥25 years ago (Guengerich et al., 1994; Shou et al., 1994; Ueng et al., 1997). Such allosteric phenomena are now generally attributed to multiple occupancy (Dabrowski et al., 2002; Schoch et al., 2004; Ekroos and Sjögren, 2006; Sohl et al., 2008; Muller et al., 2015), which can have varying effects.

Multiple occupancy, which makes kinetic simulations—and data fitting (Sohl et al., 2008)—much more complex, is beyond the scope of the modeling presented here. Moreover, the more complex a mechanism, the more ambiguous is the validity of a fit. Further, recent work has shown the relevance of conformational selection—and possibly induced fit—in the

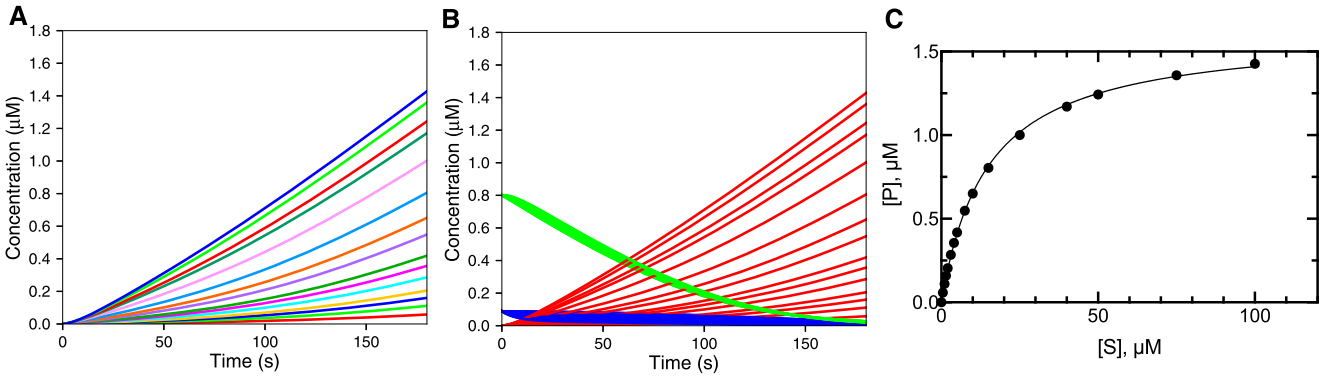

Fig. 8. Effect of consumption of an inhibitor by a different enzyme in a mixture. The model used was adapted from Figs. 1 and 7,

Step	Reaction	k_+	k_-	K_d
1	E + S ⇄ ES	1 μM^{-1} s^{-1}	10 s^{-1}	10 μM
2	ES → EP	0.1 s^{-1}	—	
3	EP ⇄ E + P	2 s^{-1}	1 μM^{-1} s^{-1}	2 μM
4	E + I ⇄ EI	1 μM^{-1} s^{-1}	0.1 s^{-1}	0.1 μM
5	F + I ⇄ FI	1 μM^{-1} s^{-1}	0.1 s^{-1}	0.10 μM
6	FI → F	0.1 s^{-1}	0	

where F is a second enzyme that does not interact with S. [E] = [F] = 0.1 μM in mixing (final concentration 0.05 μM). No premixing time was allowed to avoid consumption of I. (A) Plots of [P] versus time at varying values of [S]. (B) Time courses of [P], [I], and [EI] during course of reaction. (C) Plot of [P] formed at t = 180 seconds versus [S]. Calculations from part C yielded k_{cat} 0.0089 s^{-1} (compare with 0.0098 s^{-1} in Fig. 7A, without inhibition), $K_{m,apparent}$ = 14.7 μM, and K_i = 5.2 μM (compare with K_d of 0.1 μM for I in model). (Linear fits to Part A were poor but yielded k_{cat} = 0.0089 s^{-1}, $K_{d,apparent}$ = 85 μM, and K_i = 0.89 μM.) In Part C, the r^2 value (hyperbolic fit) was 0.9996.

substrate promiscuity of P450 enzymes (Guengerich et al., 2019a,b). Again, modeling all the details of complex P450 reactions is beyond the scope of this work, which is intended as a relatively simple primer on some issues encountered in practical drug metabolism.

In summary, we have made the following conclusions. The order of addition of substrate and inhibitors can change the apparent outcome (inhibition constant K_i), and the effect of the order is more pronounced with a stronger inhibitor. Substrate depletion alters parameters (Michaelis constant K_m) and can generate apparently sigmoidal plots. A rate-limiting step after product formation lowers the apparent K_m and distorts K_i. Consumption of an inhibitor during a reaction affects K_i and differs depending on which enzyme is involved. This work may facilitate the design and interpretation of better high-throughput assays in drug development, and these approaches can be applied readily to issues with assays of other enzymes.

Acknowledgments

Thanks are extended to Dr. M. J. Reddish for implementation of the formula for calculating k_{sp} and to K. Trisler for assistance in preparation of the manuscript.

Authorship Contributions

Participating in research design: Guengerich.
Conducted experiments: Guengerich.
Contributed new reagents or analytic tools: Guengerich.
Performed data analysis: Guengerich.
Wrote of contributed to the writing of the manuscript: Guengerich.

References

Bell LC and Guengerich FP (1997) Oxidation kinetics of ethanol by human cytochrome P450 2E1. Rate-limiting product release accounts for effects of isotopic hydrogen substitution and cytochrome b_5 on steady-state kinetics. *J Biol Chem* **272**:29643–29651.

Bell-Parikh LC and Guengerich FP (1999) Kinetics of cytochrome P450 2E1-catalyzed oxidation of ethanol to acetic acid via acetaldehyde. *J Biol Chem* **274**:23833–23840.

Buening MK, Fortner JG, Kappas A, and Corney AH (1978) 7,8-Benzoflavone stimulates the metabolic activation of aflatoxin B_1 to mutagens by human liver. *Biochem Biophys Res Commun* **82**:348–355.

Chowdhury G, Calcutt MW, and Guengerich FP (2010) Oxidation of *N*-nitrosoalkylamines by human cytochrome P450 2A6: sequential oxidation to aldehydes and carboxylic acids and analysis of reaction steps. *J Biol Chem* **285**:8031–8044.

Dabrowski MJ, Schrag ML, Wienkers LC, and Atkins WM (2002) Pyrene.pyrene complexes at the active site of cytochrome P450 3A4: evidence for a multiple substrate binding site. *J Am Chem Soc* **124**:11866–11867.

Ekroos M and Sjögren T (2006) Structural basis for ligand promiscuity in cytochrome P450 3A4. *Proc Natl Acad Sci USA* **103**:13682–13687.

Fersht A (1999) *Structure and Mechanism in Protein Science*, pp 158–161, Freeman, New York.

Fowler SM, Taylor JM, Friedberg T, Wolf CR, and Riley RJ (2002) CYP3A4 active site volume modification by mutagenesis of leucine 211. *Drug Metab Dispos* **30**:452–456.

Frank DJ, Denisov IG, and Sligar SG (2011) Analysis of heterotropic cooperativity in cytochrome P450 3A4 using α-naphthoflavone and testosterone. *J Biol Chem* **286**:5540–5545.

Guengerich FP (2014) Analysis and characterization of enzymes and nucleic acids relevant to toxicology, in *Hayes' Principles and Methods of Toxicology* (Hayes AW and Kruger CL eds) pp 1905–1964, CRC Press/Taylor & Francis, Boca Raton, FL.

Guengerich FP (2019) Inhibition of drug metabolizing enzymes, in *Handbook of Drug Metabolism* (Pearson P and Wienkers L eds) pp 222–249, CRC Press/Taylor & Francis, Boca Raton, FL.

Guengerich FP, Kim B-R, Gillam EMJ, and Shimada T (1994) Mechanisms of enhancement and inhibition of cytochrome P450 catalytic activity, in *Proceedings of the 8th International Conference on Cytochrome P450: Biochemistry, Biophysics, and Molecular Biology* (Lechner MC ed), pp 97–101, John Libbey Eurotext, Paris, France.

Guengerich FP, McCormick WA, and Wheeler JB (2003) Analysis of the kinetic mechanism of haloalkane conjugation by mammalian θ-class glutathione transferases. *Chem Res Toxicol* **16**: 1493–1499.

Guengerich FP, Miller GP, Hanna IH, Sato H, and Martin MV (2002) Oxidation of methoxyphenethylamines by cytochrome P450 2D6. Analysis of rate-limiting steps. *J Biol Chem* **277**: 33711–33719.

Guengerich FP, Müller-Enoch D, and Blair IA (1986) Oxidation of quinidine by human liver cytochrome P-450. *Mol Pharmacol* **30**:287–295.

Guengerich FP, Wilkey CJ, Glass SM, and Reddish MJ (2019a) Conformational selection dominates binding of steroids to human cytochrome P450 17A1. *J Biol Chem* **294**:10028–10041.

Guengerich FP, Wilkey CJ, and Phan TTN (2019b) Human cytochrome P450 enzymes bind drugs and other substrates mainly through conformational-selection modes. *J Biol Chem* **294**: 10928–10941.

Guest EJ, Rowland-Yeo K, Rostami-Hodjegan A, Tucker GT, Houston JB, and Galetin A (2011) Assessment of algorithms for predicting drug-drug interactions via inhibition mechanisms: comparison of dynamic and static models. *Br J Clin Pharmacol* **71**:72–87.

Hobler A, Kagawa N, Hutter MC, Hartmann MF, Wudy SA, Hannemann F, and Bernhardt R (2012) Human aldosterone synthase: recombinant expression in *E. coli* and purification enables a detailed biochemical analysis of the protein on the molecular level. *J Steroid Biochem Mol Biol* **132**:57–65.

Hosea NA and Guengerich FP (1998) Oxidation of nonionic detergents by cytochrome P450 enzymes. *Arch Biochem Biophys* **353**:365–373.

Huang MT, Johnson EF, Muller-Eberhard U, Koop DR, Coon MJ, and Conney AH (1981) Specificity in the activation and inhibition by flavonoids of benzo[*a*]pyrene hydroxylation by cytochrome P-450 isozymes from rabbit liver microsomes. *J Biol Chem* **256**: 10897–10901.

Imai T, Yamazaki T, and Kominami S (1998) Kinetic studies on bovine cytochrome p45011 beta catalyzing successive reactions from deoxycorticosterone to aldosterone. *Biochemistry* **37**: 8097–8104.

Johnson KA (2003) Introduction to kinetic analysis of enzyme systems, in *Kinetic Analysis of Macromolecules A Practical Approach* (Johnson KA ed) pp 1–18, Oxford University Press, Oxford, UK.

Johnson KA (2019) New standards for collecting and fitting steady state kinetic data. *Beilstein J Org Chem* **15**:16–29.

Korzekwa KR, Krishnamachary N, Shou M, Ogai A, Parise RA, Rettie AE, Gonzalez FJ, and Tracy TS (1998) Evaluation of atypical cytochrome P450 kinetics with two-substrate models: evidence that multiple substrates can simultaneously bind to cytochrome P450 active sites. *Biochemistry* **37**:4137–4147.

Krest CM, Onderko EL, Yosca TH, Calixto JC, Karp RF, Livada J, Rittle J, and Green MT (2013) Reactive intermediates in cytochrome p450 catalysis. *J Biol Chem* **288**:17074–17081.

Lineweaver H and Burk D (1934) The determination of enzyme dissociation constants. *J Am Chem Soc* **56**:658–666.

Ling KHJ and Hanzlik RP (1989) Deuterium isotope effects on toluene metabolism. Product release as a rate-limiting step in cytochrome P-450 catalysis. *Biochem Biophys Res Commun* **160**:844–849.

McGinnity DF, Waters NJ, Tucker J, and Riley RJ (2008) Integrated in vitro analysis for the in vivo prediction of cytochrome P450-mediated drug-drug interactions. *Drug Metab Dispos* **36**: 1126–1134.

Michaelis L and Menten ML (1913) Die Kinetik der Invertinwirkung. *Biochem Z* **49**:333–369.

Michaelis L, Menten ML, Johnson KA, and Goody RS (2011) The original Michaelis constant: translation of the 1913 Michaelis-Menten paper. *Biochemistry* **50**:8264–8269.

Michaelis L and Menten MM (2013) The kinetics of invertin action. 1913. *FEBS Lett* **587**: 2712–2720.

Müller CS, Knehans T, Davydov DR, Bounds PL, von Mandach U, Halpert JR, Caflisch A, and Koppenol WH (2015) Concurrent cooperativity and substrate inhibition in the epoxidation of carbamazepine by cytochrome P450 3A4 active site mutants inspired by molecular dynamics simulations. *Biochemistry* **54**:711–721.

Northrop DB (1998) On the meaning of K_m and *V/K* in enzyme kinetics. *J Chem Educ* **75**: 1153–1157.

Pearson PG and Wienkers LC (2019) *Handbook of Drug Metabolism*, CRC Press, Bocca Raton, FL.

Polasek TM, Shakib S, and Rostami-Hodjegan A (2018) Precision dosing in clinical medicine: present and future. *Expert Rev Clin Pharmacol* **11**:743–746.

Reddish MJ and Guengerich FP (2019) Human cytochrome P450 11B2 produces aldosterone by a processive mechanism due to the lactol form of the intermediate 18-hydroxycorticosterone. *J Biol Chem* (294):12975–12991.

Rodrigues AD and Lin JH (2001) Screening of drug candidates for their drug—drug interaction potential. *Curr Opin Chem Biol* **5**:396–401.

Sandhu P, Guo Z, Baba T, Martin MV, Tukey RH, and Guengerich FP (1994) Expression of modified human cytochrome P450 1A2 in *Escherichia coli*: stabilization, purification, spectral characterization, and catalytic activities of the enzyme. *Arch Biochem Biophys* **309**:168–177.

Sansen S, Yano JK, Reynald RL, Schoch GA, Griffin KJ, Stout CD, and Johnson EF (2007) Adaptations for the oxidation of polycyclic aromatic hydrocarbons exhibited by the structure of human P450 1A2. *J Biol Chem* **282**:14348–14355.

Schoch GA, Yano JK, Wester MR, Griffin KJ, Stout CD, and Johnson EF (2004) Structure of human microsomal cytochrome P450 2C8. Evidence for a peripheral fatty acid binding site. *J Biol Chem* **279**:9497–9503.

Schreiber G, Haran G, and Zhou HX (2009) Fundamental aspects of protein-protein association kinetics. *Chem Rev* **109**:839–860.

Segel IH (1975) Simple inhibition systems, in *Enzyme Kinetics: Behavior and Analysis of Rapid Equilibrium and Steady-State Enzyme Systems*, pp 109, John Wiley & Sons, New York.

Shou M, Grogan J, Mancewicz JA, Krausz KW, Gonzalez FJ, Gelboin HV, and Korzekwa KR (1994) Activation of CYP3A4: evidence for the simultaneous binding of two substrates in a cytochrome P450 active site. *Biochemistry* **33**:6450–6455.

Smith BD, Sanders JL, Porubsky PR, Lushington GH, Stout CD, and Scott EE (2007) Structure of the human lung cytochrome P450 2A13. *J Biol Chem* **282**:17306–17313.

Sohl CD, Isin EM, Eoff RL, Marsch GA, Stec DF, and Guengerich FP (2008) Cooperativity in oxidation reactions catalyzed by cytochrome P450 1A2: highly cooperative pyrene hydroxylation and multiphasic kinetics of ligand binding. *J Biol Chem* **283**:7293–7308.

Ueng Y-F, Kuwabara T, Chun YJ, and Guengerich FP (1997) Cooperativity in oxidations catalyzed by cytochrome P450 3A4. *Biochemistry* **36**:370–381.

Wakayama N, Toshimoto K, Maeda K, Hotta S, Ishida T, Akiyama Y, and Sugiyama Y (2018) In silico prediction of major clearance pathways of drugs among 9 routes with two-step support vector machines. *Pharm Res* **35**:197.

Walsh C (1979) *Enzymatic Reaction Mechanisms*, pp 67–71, W. H. Freeman, San Francisco, CA.

Wang A, Savas U, Stout CD, and Johnson EF (2011) Structural characterization of the complex between alpha-naphthoflavone and human cytochrome P450 1B1. *J Biol Chem* **286**:5736–5743.

Wiebel FJ, Leutz JC, Diamond L, and Gelboin HV (1971) Aryl hydrocarbon (benzo(*a*)pyrene) hydroxylase in microsomes from rat tissues: differential inhibition and stimulation by benzoflavones and organic solvents. *Arch Biochem Biophys* **144**:78–86.

Wienkers LC and Heath TG (2005) Predicting in vivo drug interactions from in vitro drug discovery data. *Nat Rev Drug Discov* **4**:825–833.

Zang H, Fang Q, Pegg AE, and Guengerich FP (2005) Kinetic analysis of steps in the repair of damaged DNA by human O^6-alkylguanine-DNA alkyltransferase. *J Biol Chem* **280**:30873–30881.

Zhang D, Zhu M, and Humphreys WG (2008) *Drug Metabolism in Drug Design and Development: Basic Concepts and Practice*, Wiley, Hoboken, NJ.

Address correspondence to: Dr. F. Peter Guengerich, Department of Biochemistry, Vanderbilt University School of Medicine, 638B Robinson Research Building, 2200 Pierce Avenue, Nashville, Tennessee 37232-0146. E-mail: f.guengerich@vanderbilt.edu

SUPPORTING INFORMATION

Kinetic Modeling of Steady-State Situations in Cytochrome P450 Enzyme Reactions

F. Peter Guengerich

TABLE OF CONTENTS

Fig. S1

A

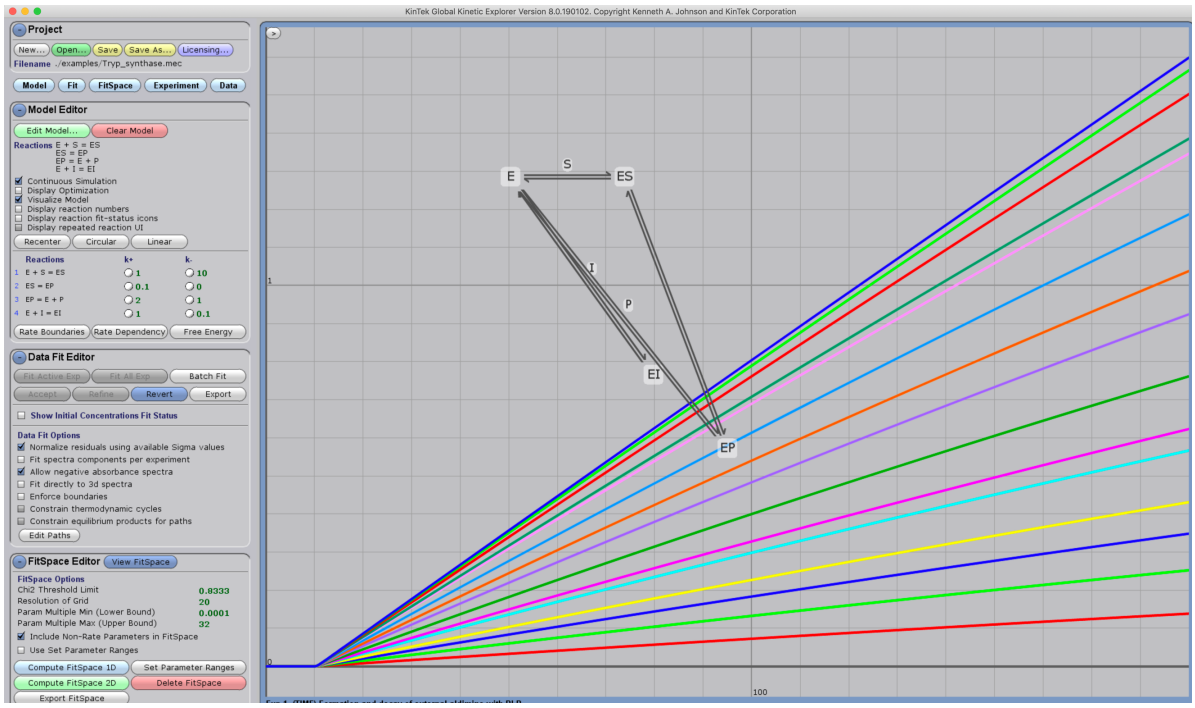
KinTek Global Kinetic Explorer Version 8.0.190102. Copyright Kenneth A. Johnson and KinTek Corporation
Project
Model Editor
Data Fit Editor
FitSpace Editor
E
S
ES
I
P
EI
EP
100

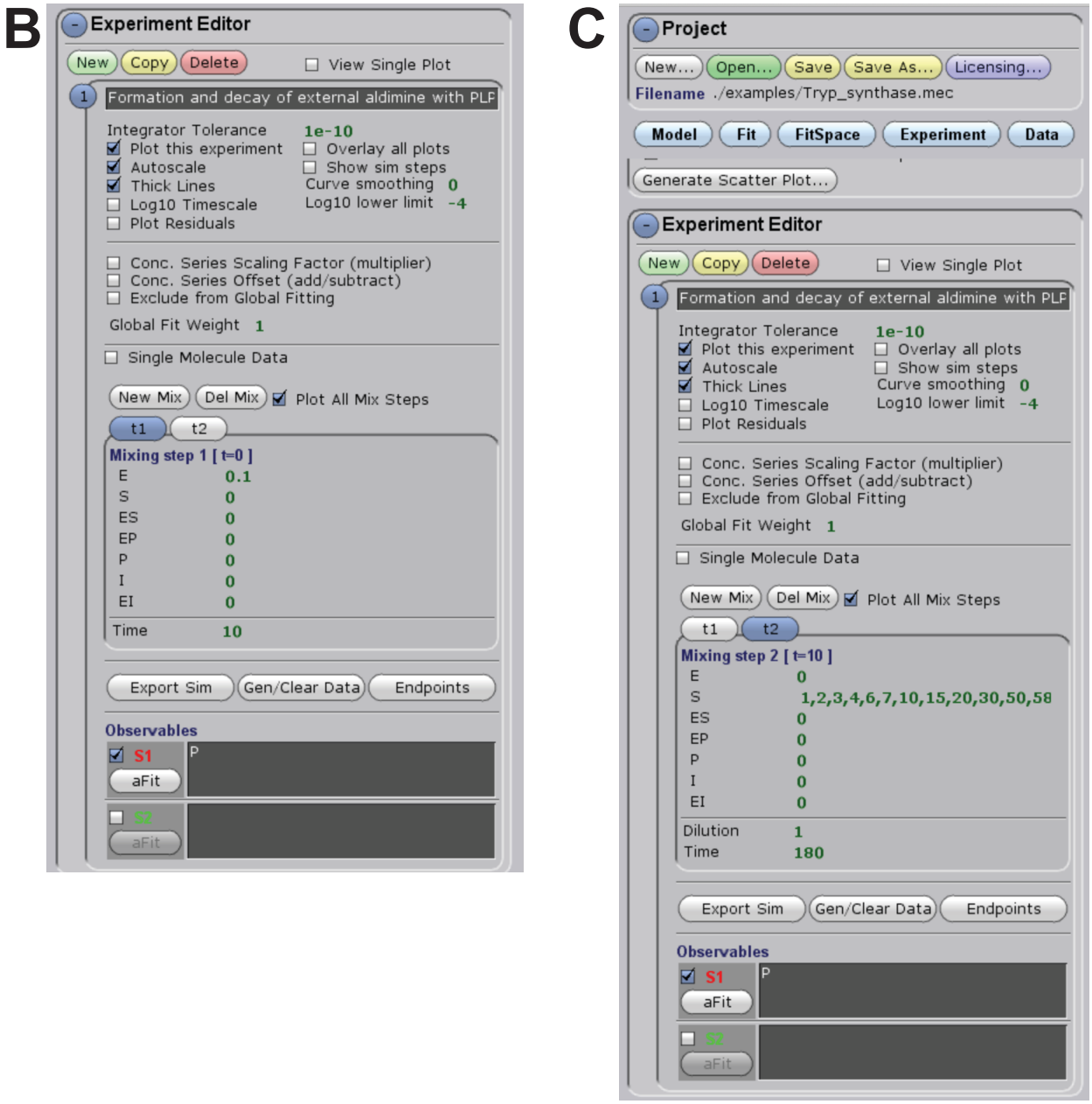

Fig. S1. Screenshot of KinTek Explorer® setup for the modeling in Fig. 1A. The three parts (A, B, C) show poses in the screen to indicate the basic setup.

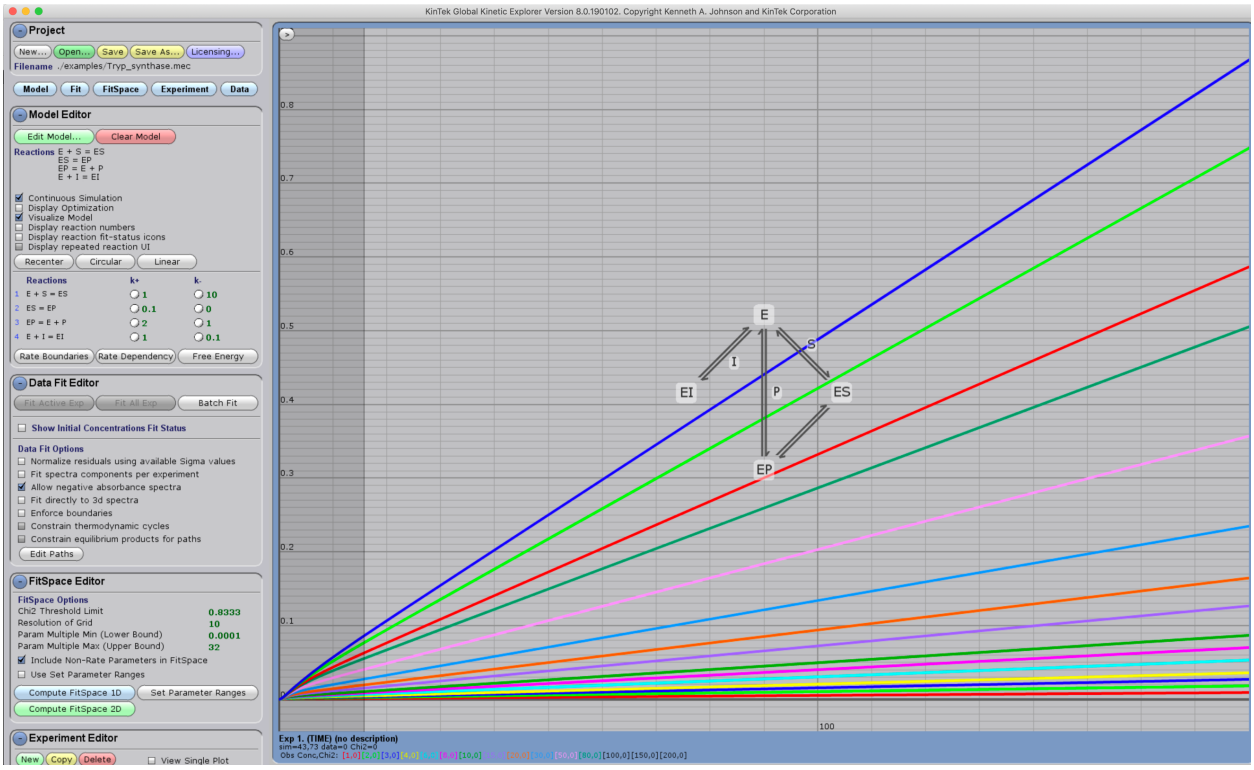

Fig. S2. Screenshot of KinTek Explorer® model for experiment of Fig. 1B. See parameters under Model Editor. Units are in μM and seconds (s^{-1} for first order reactions and μM^{-1} s^{-1} for second order reactions). A "=" symbol indicates a reversible reaction, and a back reaction rate constant of zero is used to make a reaction irreversible.

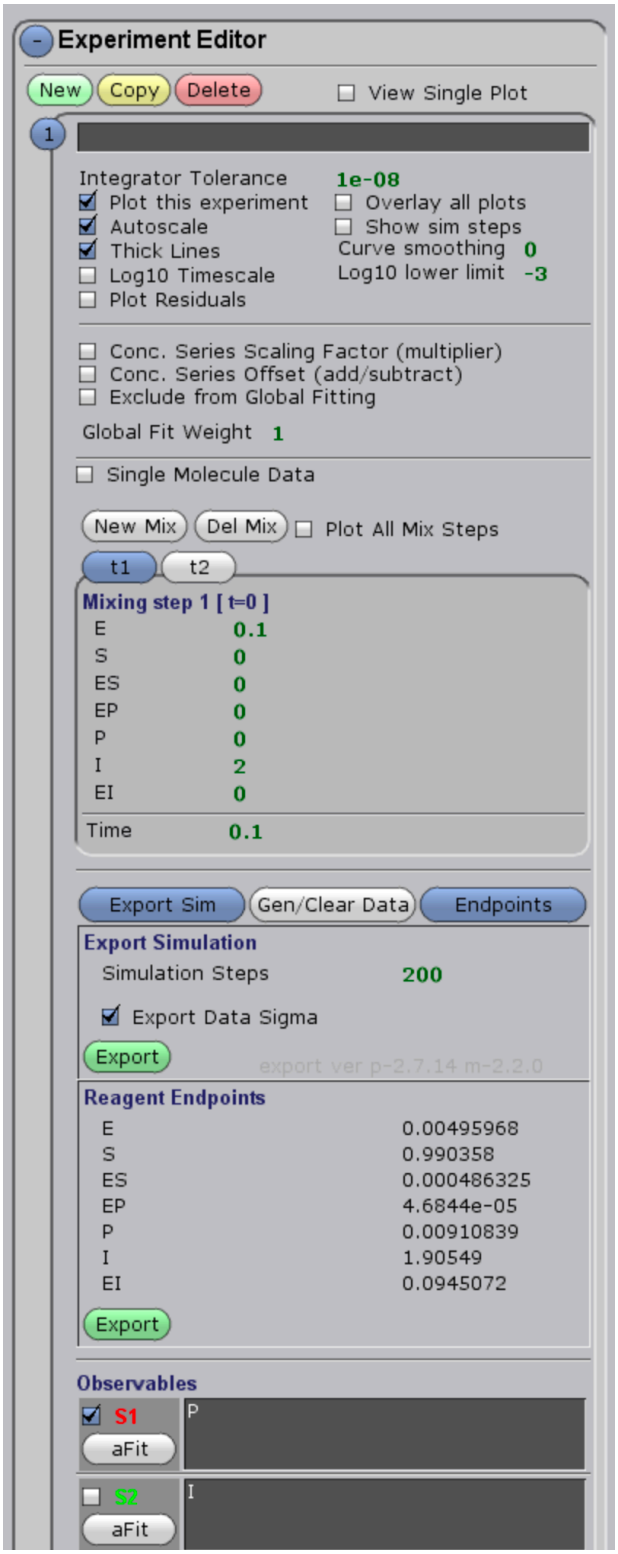

Fig. S3. Step t_1 for the reaction model (Fig. 1B) shown in Fig. S1.

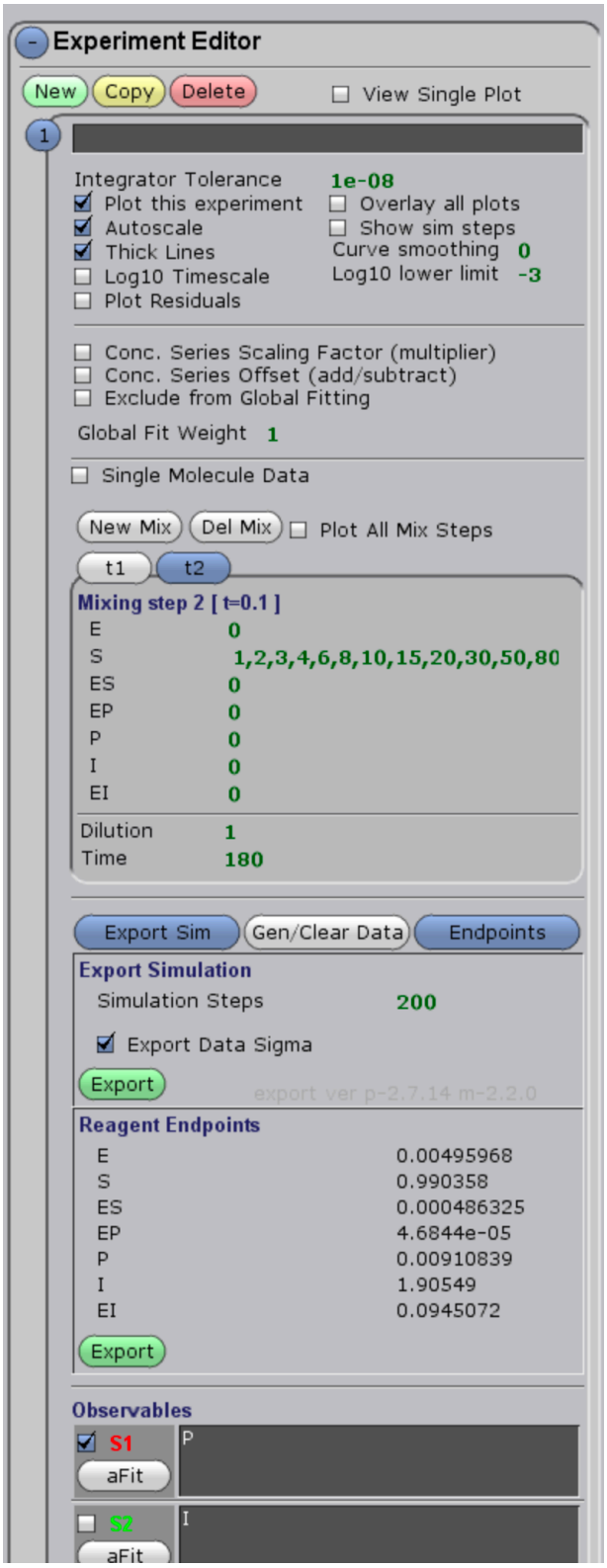

Fig. S4. Step t_2 for the reaction mode (Fig. 1B) shown in Fig. S1.

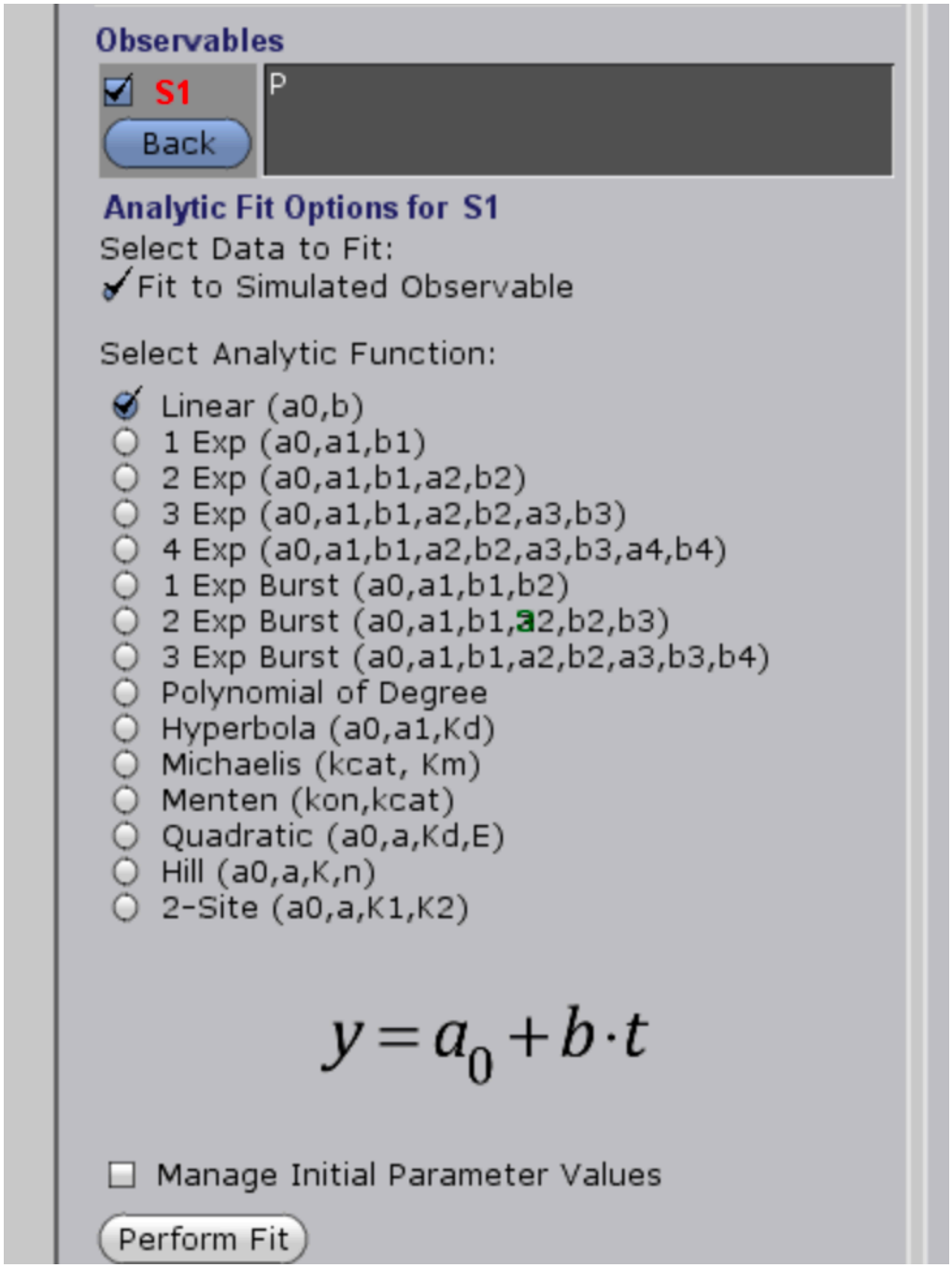

Fig. S5. Observables (Analytic Fit option) for analyzing the reaction model (Fig. 1B) in Fig. S1.

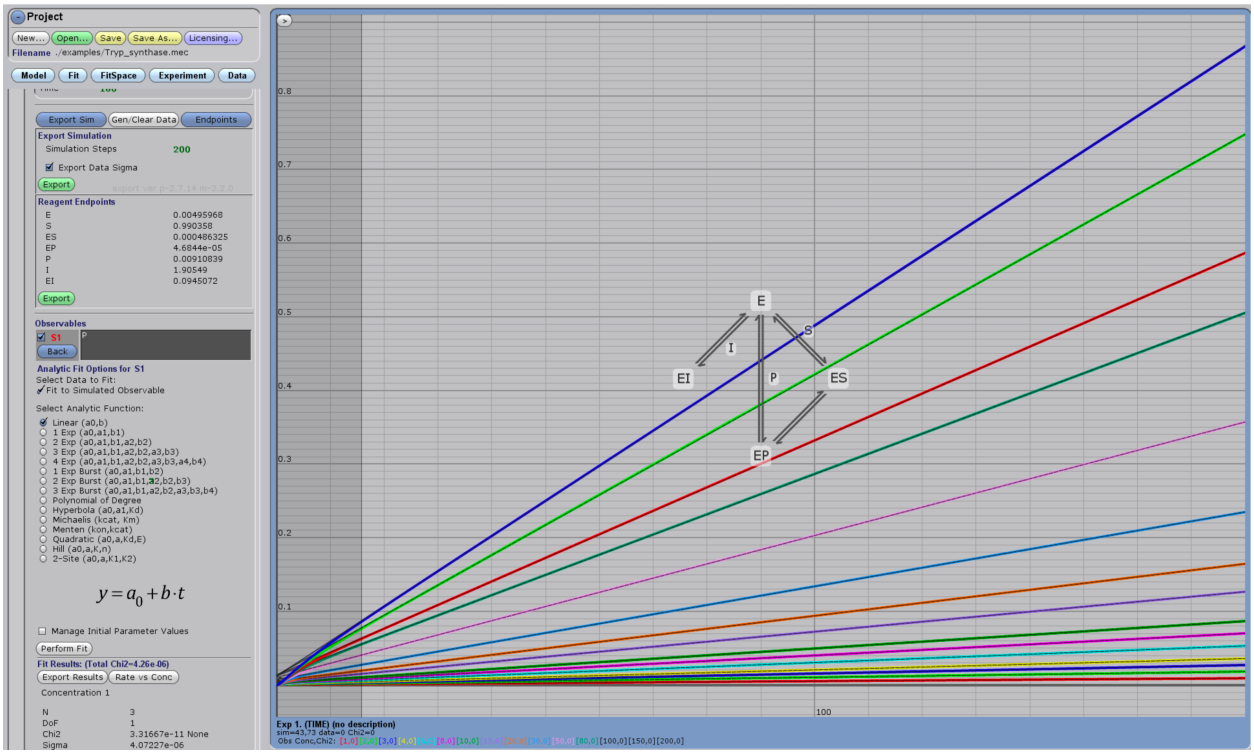

Fig. S6. Linear fitting of plots in Fig. S1.

Fig. S7

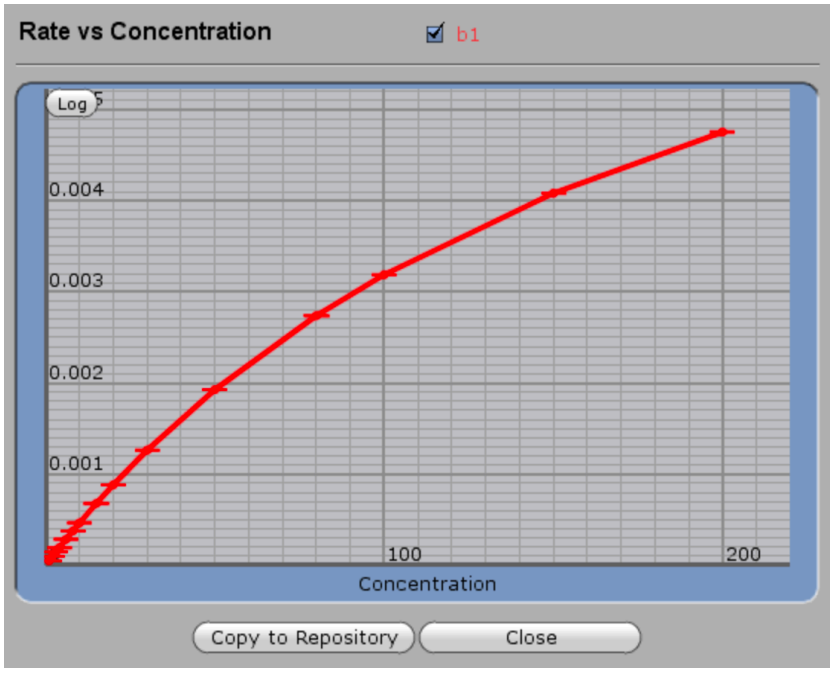

Fig. S7. Plot of <Rate *vs*. Conc> from rates obtained in Fig. S5 (Hyperbola). Alternatively <Michaelis> could have been selected to obtain the same result.

Fig. S8

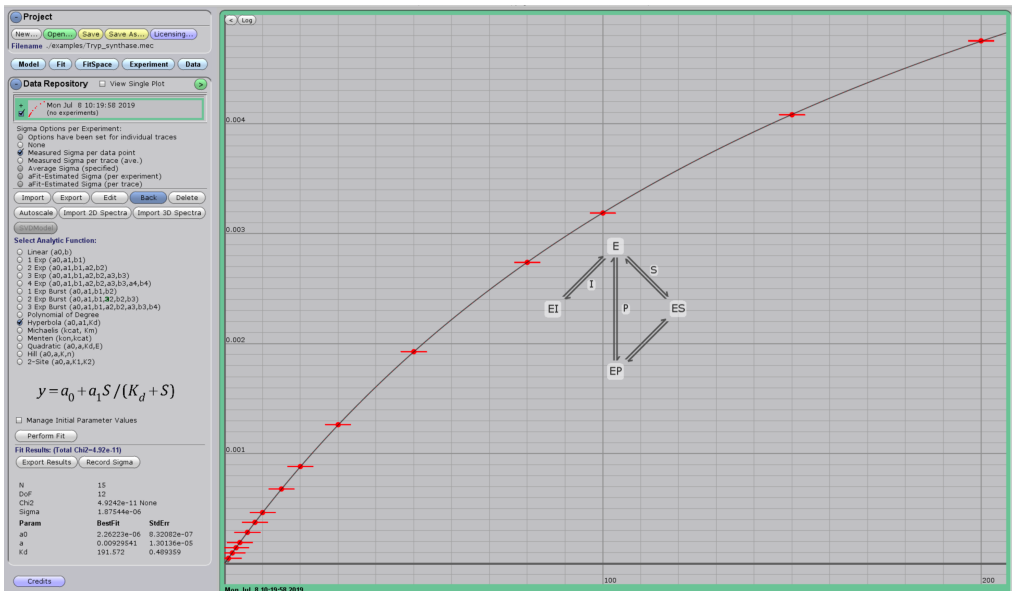

Fig. S8. Selected fit from Fig. S6 (following <Copy to Repository> in the step in Fig. S6).